EPJ Web of Conferences **20**, 02008 (2012)
DOI: 10.1051/epjconf/20122002008

Interactions and decays of high-spin baryon resonances

Yongseok Oh[a]

Department of Physics, Kyungpook National University, Daegu 702-701, Korea

Abstract. Understanding strong interactions at low energy region requires the precise knowledge on the spectra and the properties of hadrons. Such informations can be obtained through detailed and sophisticated analyses of experimental data collected from various scattering processes using electromagnetic beams or hadron beams. At present, there have been a lot of precise data collected for the production of meson-baryon final states in photon-nucleon and nucleon-nucleon scattering processes. Since the total center-of-mass energy range of such scattering experiments covers the resonance region of about 2 GeV, it is legitimate to include as many baryon resonances as possible in the analyses of the data, which requires the formalism to describe high-spin baryon resonances. Here, we use the Fronsdal method to describe high-spin baryon resonances and develop their interaction Lagrangians. We then apply this method to investigate the role of high-spin baryon resonances in the reactions of $\gamma p \to K\Sigma(1385)$ and $\gamma p \to K^+K^+\Xi^-$.

1 Introduction

The properties of baryons reflect the strong interaction at low energy region. The underlying theory of strong interaction in the standard model is Quantum Chromodynamics (QCD). In spite of the success of QCD at high energies, however, application of QCD to low energy region is still far from complete. Therefore, investigation of the spectrum and the properties of baryons relies on phenomenological models of QCD such as quark models, bag models, soliton models, etc. Those models enjoy success to describe major properties of baryons, but the success is mostly limited to the ground states of baryons.

Listed in the Particle Data Group (PDG) are about 20 nucleon resonances, about 20 Δ resonances, and more than 20 hyperon resonances with strangeness $S = -1$ [1]. However, most phenomenological models predict much richer structure of baryon spectrum and, furthermore, most of the properties of baryon resonances are still poorly understood. Baryon resonances are produced in photon-nucleon or nucleon-nucleon scattering experiments and then decay very quickly to stable particles, for example, to the πN channel. Furthermore, most baryon resonances have large decay widths, which makes it difficult to find them in experiments. Thus it requires detailed and sophisticated analyses of data to confirm the existence of baryon resonances as well as to constrain their properties.

Most of the confirmed baryon resonances have been found in the πN channel and many efforts have been devoted to search for baryon resonances in the other channels. Confirming the known baryon resonances in other channels is also desirable since their partial decay widths can be determined, which can reveal the dynamics of quarks and gluons through the structures of the resonances.

However, in the resonance region of around 2 GeV, many resonances have high spin ($j > 3/2$). Therefore, it is necessary to include such high-spin resonances to extract more reliable information on the resonances from the experimental data and the efforts are already started to treat higher-spin resonances. (See, for example, Refs. [2–5].) However, most works are limited by employing only a few interaction terms, and, furthermore, it is hard to compare the extracted coupling constants to the predictions of phenomenological models for hadron structure.

[a] e-mail: yohphy@knu.ac.kr

In this work, we use a general formalism to treat high-spin baryon resonances by adopting the method developed by Fronsdal *et al.* based on the Rarita-Schwinger formalism. This includes the most general forms of the effective Lagrangians describing the interactions of baryon resonances. To be specific, we work with the reactions of $\gamma p \to K\Sigma(1385)$ and $\gamma p \to K^+K^+\Xi^-$. By doing this, we also derive relations between the coupling constants of the interaction Lagrangians and the predictions of quark models.

In the next Section, we summarize the forms of the propagators of baryons fields, which are obtained by using the method of Fronsdal [6,7]. In Sect. 3 and 4, we apply this method to analyze the reactions of $\gamma p \to K\Sigma(1385)$ and $\gamma p \to K^+K^+\Xi^-$, which shows the important role of high-spin resonances in the production mechanisms. The explicit forms for effective Lagrangians are given and the comparison with a quark model is made, if possible. Section 5 contains a summary and a discussion.

2 Propagators of Baryons

The formalism for the propagator of an arbitrary spin field can be obtained following the schemes of Refs. [6–9], when the field is on its mass-shell. Referring the detail to Refs. [6–9], we here briefly give the results for the propagators.

In the Rarita-Schwinger formalism [10], a fermion field of spin j is represented by a tensor of rank $n = j - 1/2$, which satisfies the free field equation,

$$(i\partial\!\!\!/ - M)\, R_{\alpha_1\cdots\alpha_n} = 0, \tag{1}$$

where M is the mass of the fermion. The field also satisfies the subsidiary conditions,

$$p^{\alpha_1} R_{\alpha_1\alpha_2\cdots\alpha_n} = 0, \qquad g^{\alpha_1\alpha_2} R_{\alpha_1\alpha_2\cdots\alpha_n} = 0, \qquad \gamma^{\alpha_1} R_{\alpha_1\alpha_2\cdots\alpha_n} = 0. \tag{2}$$

Then, for a fermion field of spin j, mass M and momentum p, the propagator can be written as

$$S(p) = \frac{1}{p^2 - M^2}\left(p\!\!\!/ + M\right) \Delta^{\beta_1\cdots\beta_n}_{\alpha_1\cdots\alpha_n}(j,p). \tag{3}$$

We first define

$$\bar{g}_{\mu\nu} = g_{\mu\nu} - \frac{1}{M^2} p_\mu p_\nu, \qquad \bar{\gamma}^\mu = \gamma^\mu - \frac{1}{M^2} p\!\!\!/ p^\mu. \tag{4}$$

Then we have

$$\Delta(\tfrac{1}{2}, p) = 1, \tag{5}$$

$$\begin{aligned}\Delta^{\beta_1}_{\alpha_1}(\tfrac{3}{2}, p) &= -\left(\bar{g}^{\beta_1}_{\alpha_1} - \frac{1}{3}\bar{\gamma}_{\alpha_1}\bar{\gamma}^{\beta_1}\right) \\ &= -g^{\beta_1}_{\alpha_1} + \frac{1}{3}\gamma_{\alpha_1}\gamma^{\beta_1} + \frac{1}{3M}\left(\gamma_{\alpha_1} p^{\beta_1} - p_{\alpha_1}\gamma^{\beta_1}\right) + \frac{2}{3M^2} p_{\alpha_1} p^{\beta_1},\end{aligned} \tag{6}$$

$$\begin{aligned}\Delta^{\beta_1\beta_2}_{\alpha_1\alpha_2}(\tfrac{5}{2}, p) &= \frac{1}{2}\left(\bar{g}^{\beta_1}_{\alpha_1}\bar{g}^{\beta_2}_{\alpha_2} + \bar{g}^{\beta_2}_{\alpha_1}\bar{g}^{\beta_1}_{\alpha_2}\right) - \frac{1}{5}\bar{g}_{\alpha_1\alpha_2}\bar{g}^{\beta_1\beta_2} \\ &\quad - \frac{1}{10}\left(\bar{\gamma}_{\alpha_1}\bar{\gamma}^{\beta_1}\bar{g}^{\beta_2}_{\alpha_2} + \bar{\gamma}_{\alpha_1}\bar{\gamma}^{\beta_2}\bar{g}^{\beta_1}_{\alpha_2} + \bar{\gamma}_{\alpha_2}\bar{\gamma}^{\beta_1}\bar{g}^{\beta_2}_{\alpha_1} + \bar{\gamma}_{\alpha_2}\bar{\gamma}^{\beta_2}\bar{g}^{\beta_1}_{\alpha_1}\right),\end{aligned} \tag{7}$$

$$\begin{aligned}\Delta^{\beta_1\beta_2\beta_3}_{\alpha_1\alpha_2\alpha_3}(\tfrac{7}{2}, p) &= \frac{4}{9}\gamma^\alpha\gamma_\beta \Delta^{\beta\beta_1\beta_2\beta_3}_{\alpha\alpha_1\alpha_2\alpha_3}(4,p) \\ &= -\frac{1}{36}\sum_{P(\alpha),P(\beta)}\left\{\bar{g}^{\beta_1}_{\alpha_1}\bar{g}^{\beta_2}_{\alpha_2}\bar{g}^{\beta_3}_{\alpha_3} - \frac{3}{7}\bar{g}^{\beta_1}_{\alpha_1}\bar{g}_{\alpha_2\alpha_3}\bar{g}^{\beta_2\beta_3} - \frac{3}{7}\bar{\gamma}_{\alpha_1}\bar{\gamma}^{\beta_1}\bar{g}^{\beta_2}_{\alpha_2}\bar{g}^{\beta_3}_{\alpha_3} + \frac{3}{35}\bar{\gamma}_{\alpha_1}\bar{\gamma}^{\beta_1}\bar{g}_{\alpha_2\alpha_3}\bar{g}^{\beta_2\beta_3}\right\},\end{aligned} \tag{8}$$

where $\sum_{P(\alpha),P(\beta)}$ means the sum over all possible permutations of α_i's and β_i's. The propagators of higher spin baryon fields can be read straightforwardly by using the methods given in Refs. [6–9].

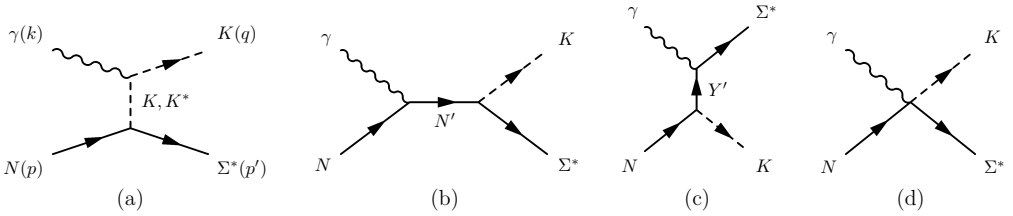

Fig. 1. Feynman diagrams for $K\Sigma^*$ photoproduction. N' stands for the non-strange baryons and their resonances, while Y' the hyperons with strangeness -1 and their resonances. Diagram (d) includes the contact term of which form can be found in Ref. [11].

The interaction Lagrangian of baryon resonances with other hadrons can be constructed by making use of the parity conservation and angular momentum conservation, etc. The number of possible couplings is determined by these symmetries. In principle, the coupling constants appearing in the effective Lagrangian can be estimated by the models on hadron structure or be fitted by experimental data for scattering processes. In the next Sections, we give the explicit forms for the effective Lagrangians that are needed in the analyses of $\gamma p \to K\Sigma(1385)$ and $\gamma p \to K^+K^+\Xi^-$ and discuss how to constrain the coupling constants in the effective Lagrangian.

3 The Reaction of $\gamma p \to K\Sigma(1385)$

We first consider the reaction of $K\Sigma(1385)$ photoproduction, i.e., $\gamma p \to K^+\Sigma^0(1385)$ and $\gamma n \to K^+\Sigma^-(1385)$ [11]. In particular, we consider the resonance energy region for investigating the role of the nucleon and Δ resonances of masses around 2 GeV and for constraining the physical parameters of those resonances. This reaction is expected to have a non-negligible role in searching for missing resonances. In a naive consideration, the cross sections of this reaction are smaller than those of $K\Lambda(1116)$ and of $K\Sigma(1193)$ photoproduction. Although this expectation is confirmed by recent experiments [12,13], the suppression is found to be not so large contrary to the naive expectation, which implies a potential role of baryon resonances in its production mechanisms. In fact, in the quark model of Ref. [14], several missing or not-well-established baryon resonances are predicted to have strong couplings to this channel. Therefore, it would be useful to investigate the role of such resonances in the production mechanisms of $K\Sigma(1385)$ photoproduction.

Our model for this process is shown in Fig. 1, which includes the t-channel K and K^* meson exchanges and intermediate nucleon/Δ and hyperon resonances. It also includes the generalized contact term that is required to restore gauge invariance. The details for the effective Lagrangians that are needed for the t-channel K meson exchange, the s-channel nucleon term, the u-channel $\Lambda(1116)$ term, the u-channel $\Sigma(1385)$ term, and the contact term can be found in Ref. [11]. Here, we focus on the Lagrangians which include interactions with higher spin resonances.

Since the $\Sigma(1385)$ has spin-3/2, we first consider the $K^*N\Sigma^*$ interaction, which describes the vertex of $\frac{3}{2} \to 1 + \frac{1}{2}$, where the numbers represent the spin of the involved particles. The most general form of this interaction contains three couplings and are written as

$$\mathcal{L}_{K^*N\Sigma^*} = \frac{ig_1}{2M_N}\overline{K}^{*\mu\nu}\overline{\boldsymbol{\Sigma}}^*_\mu \cdot \boldsymbol{\tau}\gamma_\nu\gamma_5 N + \frac{g_2}{(2M_N)^2}\overline{K}^{*\mu\nu}\overline{\boldsymbol{\Sigma}}^*_\mu \cdot \boldsymbol{\tau}\gamma_5\partial_\nu N - \frac{g_3}{(2M_N)^2}\partial_\nu\overline{K}^{*\mu\nu}\overline{\boldsymbol{\Sigma}}^*_\mu \cdot \boldsymbol{\tau}\gamma_5 N + \text{ H.c.}, \quad (9)$$

where $K^*_{\mu\nu} = \partial_\mu K^*_\nu - \partial_\nu K^*_\mu$. The three coupling constants are not determined directly from experiments, and we use the SU(3) relations to estimate the strengths of these couplings from the corresponding $\rho N\Delta$ interaction. However, this can be done only for g_1 as the previous works were based on the Lagrangian which has only the g_1 term [15,16]. Therefore, here, we assume that $g_2 \approx g_3 \approx 0$. We could justify this assumption by confirming that the contributions from the g_2 and the g_3 terms are negligible unless they are extraordinarily large.

Since one of the motivation of this study is to investigate the role of the non-strange baryon resonances in the s-channel diagrams, we begin with the most general expressions for the interactions of

Resonance	**PDG** [1]	h_1	h_2	f_1	f_2
$N\frac{1}{2}^-(1945)$	$S_{11}^*(2090)$	−0.98	—	0.055	—
$N\frac{3}{2}^-(1960)$	$D_{13}^{**}(2080)$	0.24	−0.54	−1.25	1.21
$N\frac{5}{2}^-(2095)$	$D_{15}^{**}(2200)$	0.29	−0.08	0.37	0.28
$\Delta\frac{3}{2}^-(2080)$	$D_{33}^{*}(1940)$	−0.68	1.00	0.39	−0.57
$\Delta\frac{5}{2}^+(1990)$	$F_{35}^{**}(2000)$	−0.87	0.11	−0.68	−0.062
$N\frac{3}{2}^-(2095)$		0.99	0.27	0.49	−0.83
$N\frac{5}{2}^+(1980)$		0.59	0.24	0.019	−0.13
$\Delta\frac{3}{2}^-(2145)$		0.25	0.46	0.11	−0.059

Table 1. Resonances and their coupling constants h_i and f_i based on the predictions of Ref. [14]. The coupling constants are calculated using the resonance masses of PDG.

$RN\gamma$ and $RK\Sigma^*$, where R stands for a baryon resonance. They are obtained as

$$\begin{aligned}
\mathcal{L}_{RN\gamma}(\tfrac{1}{2}^\pm) &= \frac{ef_1}{2M_N}\bar{N}\Gamma^{(\mp)}\sigma_{\mu\nu}\partial^\nu A^\mu R + \text{H.c.},\\
\mathcal{L}_{RN\gamma}(\tfrac{3}{2}^\pm) &= -\frac{ief_1}{2M_N}\overline{N}\Gamma_\nu^{(\pm)}F^{\mu\nu}R_\mu - \frac{ef_2}{(2M_N)^2}\partial_\nu\bar{N}\Gamma^{(\pm)}F^{\mu\nu}R_\mu + \text{H.c.},\\
\mathcal{L}_{RN\gamma}(\tfrac{5}{2}^\pm) &= \frac{ef_1}{(2M_N)^2}\bar{N}\Gamma_\nu^{(\mp)}\partial^\alpha F^{\mu\nu}R_{\mu\alpha} - \frac{ief_2}{(2M_N)^3}\partial_\nu\bar{N}\Gamma^{(\mp)}\partial^\alpha F^{\mu\nu}R_{\mu\alpha} + \text{H.c.},
\end{aligned} \tag{10}$$

and

$$\begin{aligned}
\mathcal{L}_{RK\Sigma^*}(\tfrac{1}{2}^\pm) &= \frac{h_1}{M_K}\partial_\mu K\bar{\Sigma}^{*\mu}\Gamma^{(\mp)}R + \text{H.c.},\\
\mathcal{L}_{RK\Sigma^*}(\tfrac{3}{2}^\pm) &= \frac{h_1}{M_K}\partial^\alpha K\bar{\Sigma}^{*\mu}\Gamma_\alpha^{(\pm)}R_\mu + \frac{ih_2}{M_K^2}\partial^\mu\partial^\alpha K\bar{\Sigma}_\alpha^*\Gamma^{(\pm)}R_\mu + \text{H.c.},\\
\mathcal{L}_{RK\Sigma^*}(\tfrac{5}{2}^\pm) &= \frac{ih_1}{M_K^2}\partial^\mu\partial^\beta K\bar{\Sigma}^{*\alpha}\Gamma_\mu^{(\mp)}R_{\alpha\beta} - \frac{h_2}{M_K^3}\partial^\mu\partial^\alpha\partial^\beta K\bar{\Sigma}_\mu^*\Gamma^{(\mp)}R_{\alpha\beta} + \text{H.c.}.
\end{aligned} \tag{11}$$

where A_μ is the photon field and its field strength tensor is $F_{\mu\nu} = \partial_\mu A_\nu - \partial_\nu A_\mu$). Here, R, R_μ, and $R_{\mu\nu}$ are the baryon fields for the spin-1/2, 3/2, and 5/2 resonances, respectively, with

$$\Gamma_\mu^{(\pm)} = \begin{pmatrix}\gamma_\mu\gamma_5\\ \gamma_\mu\end{pmatrix}, \qquad \Gamma^{(\pm)} = \begin{pmatrix}\gamma_5\\ \mathbf{1}\end{pmatrix}. \tag{12}$$

The coupling constants f_i and h_i can be related to the theoretical predictions on the partial decay amplitudes of the resonances. This has a great advantage compared with the use of partial decay widths as the relative phase of the coupling constants can be fixed. For example, for the case of spin-3/2 resonance with positive parity, the decay amplitudes can be obtained as

$$\begin{aligned}
G(1) &= G_{11}^{(3/2)}\frac{h_1}{M_K} + G_{12}^{(3/2)}\frac{h_2}{M_K^2},\\
G(3) &= G_{31}^{(3/2)}\frac{h_1}{M_K} + G_{32}^{(3/2)}\frac{h_2}{M_K^2},
\end{aligned} \tag{13}$$

for a positive parity resonance, where

$$\begin{aligned}
G_{11}^{(3/2)} &= \frac{\sqrt{30}}{60\sqrt{\pi}}\frac{1}{M_{\Sigma^*}}\sqrt{\frac{q}{M_R}}\sqrt{E_{\Sigma^*}-M_{\Sigma^*}}(M_R+M_{\Sigma^*})(E_{\Sigma^*}+4M_{\Sigma^*}),\\
G_{12}^{(3/2)} &= -\frac{\sqrt{30}}{60\sqrt{\pi}}\frac{q^2\sqrt{qM_R}}{M_{\Sigma^*}}\sqrt{E_{\Sigma^*}-M_{\Sigma^*}}
\end{aligned}$$

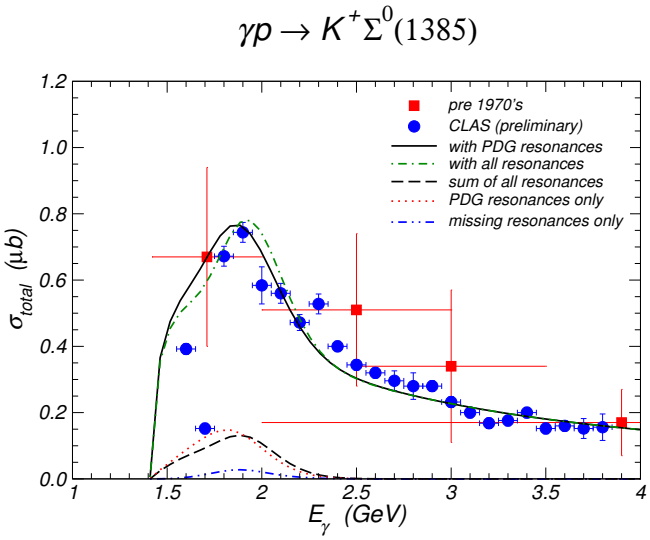

Fig. 2. Total cross sections for the $\gamma p \to K^+\Sigma^0(1385)$ reaction with the resonance parameters listed in Table 1.

$$G_{31}^{(3/2)} = -\frac{\sqrt{30}}{20\sqrt{\pi}}\frac{1}{M_{\Sigma^*}}\sqrt{\frac{q}{M_R}}\sqrt{E_{\Sigma^*}-M_{\Sigma^*}}(M_R+M_{\Sigma^*})(E_{\Sigma^*}-M_{\Sigma^*}),$$
$$G_{32}^{(3/2)} = \frac{\sqrt{30}}{20\sqrt{\pi}}\frac{q^2\sqrt{qM_R}}{M_{\Sigma^*}}\sqrt{E_{\Sigma^*}-M_{\Sigma^*}}, \tag{14}$$

where

$$q = \frac{1}{2M_R}\sqrt{\left[M_R^2-(M_{\Sigma^*}+M_K)^2\right]\left[M_R^2-(M_{\Sigma^*}-M_K)^2\right]}, \tag{15}$$

and $E_{\Sigma^*} = \sqrt{M_{\Sigma^*}^2+q^2}$. The decay amplitudes are predicted by the quark model of Ref. [14], which allows us to determine the coupling constants of our effective Lagrangians. The explicit formulas for the other resonances can be found in Ref. [11], and the couplings fixed by the quark model prediction of Refs. [14] are listed in Table 1.In this work, only the resonances that are predicted to have large couplings to the $K\Sigma^*$ channel in the model of Ref. [14] are considered.

In Fig. 2, we present the results for the total cross sections for the $\gamma p \to K^+\Sigma^0(1385)$ reaction. This evidently shows the nontrivial role of the baryon resonances in this reaction. In particular, the nontrivial contributions from the $\Delta(2000)F_{35}$, the $\Delta(1940)D_{33}$, and the $N(2080)D_{13}$, as well as from the missing resonance $N\frac{3}{2}^-(2095)$, are found to be essential to describe the measured data of Ref. [12].

The same model is then applied to the reaction of $\gamma n \to K^+\Sigma^-(1385)$ with keeping the same resonances and respecting the isospin symmetry. The predictions of this model for differential cross sections and beam asymmetry are compared with the data obtained by the LEPS Collaboration [13] in Fig. 3. Considering that only a few resonances are included and no additional free parameters are allowed, the description of this model for the differential cross sections is reasonable. However, the difficulty in explaining the beam asymmetry indicates that more sophisticated and detailed analyses of the data are highly required to further constrain the physical parameters of baryon resonances.

4 The Reaction of $\gamma p \to K^+K^+\Xi^-$

In this Section, we apply the previous formalism to the reaction of $\gamma p \to K^+K^+\Xi^-$. For the model to describe the $\gamma p \to K^+K^+\Xi^-$ reaction, we consider the diagrams shown in Fig. 4 [17,18]. As discussed in Ref. [17], the main contribution comes from the excitation of intermediate hyperons because of the

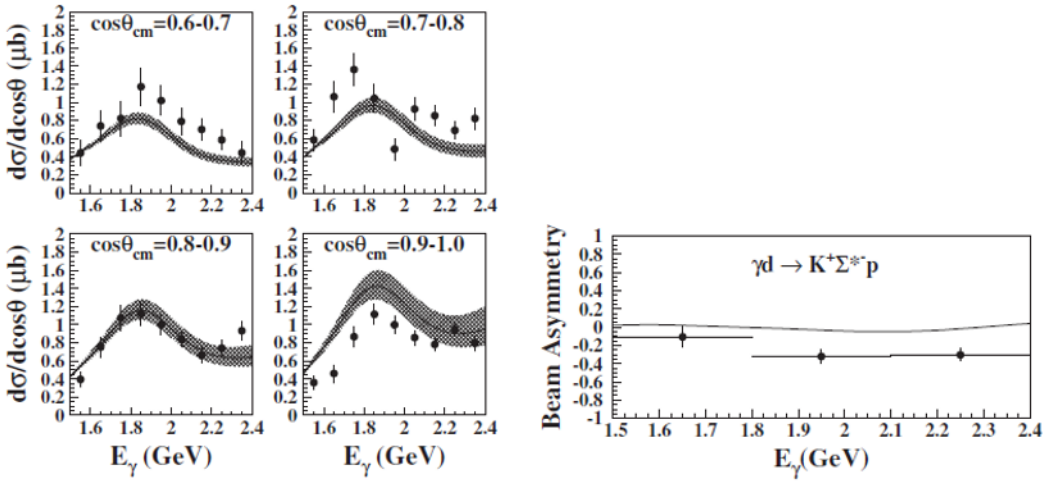

Fig. 3. (Left panel) Differential cross sections for the $\gamma n \to K^+\Sigma^-(1385)$ reaction with the resonances listed in Table 1. (Right panel) Beam asymmetry of the same reaction. The data are from Ref. [13].

absence of exotic mesons having strangeness $S = 2$. This feature is very different from the reaction mechanisms of $\gamma N \to K\bar{K}N$, where the dominant contribution comes from the production of the ϕ meson [16]. Therefore, Ξ production is a very useful tool to investigate hyperon resonances having $S = -1$.

There are many Λ and Σ resonances [1] that may have a crucial role in this process. In the model of Ref. [17], as a first trial, lower mass hyperon resonances of spin 1/2 and 3/2 have been considered. It was, then, found that this model predicts a bump structure in the $K^+\Xi^-$ invariant mass distribution while such a structure was not seen in the experimental data [19]. This is because of the absence of hyperon resonances that has a mass around 2 GeV with spin 1/2 or 3/2 and it was shown in Ref. [17], that inclusion of a resonance of this mass range may resolve the problem. However, in PDG, there is no hyperon resonances of spin 1/2 or 3/2 in this mass region. Instead, such resonances are found to have spin 5/2 or 7/2 [1].

It is, therefore, necessary to include high-spin hyperon resonances in order to understand the production mechanisms of Ξ photoproduction. In Ref. [18], the relevant effective Lagrangians are constructed as

$$\begin{aligned}
\mathcal{L}^{5/2^\pm}_{BYK} &= i\frac{g_{BYK}}{m_K^2}\bar{B}\Gamma^{(\pm)}Y^{\mu\nu}\partial_\mu\partial_\nu\bar{K} + \text{ H.c.},\\
\mathcal{L}^{5/2^\pm}_{BYK\gamma} &= -\frac{g_{BYK}}{m_K^2}\hat{e}_K\bar{B}\Gamma^{(\pm)}Y^{\mu\nu}\left(A_\mu\partial_\nu + \partial_\nu A_\nu\right)\bar{K} + \text{ H.c.},
\end{aligned} \tag{16}$$

for spin 5/2 hyperon Y, where B is a spin 1/2 baryon field. Here, the latter is obtained from the former by minimal substitution and $\hat{e}_K$ is the charge of the K meson. The corresponding Lagrangian for a spin-$7/2$ hyperon resonance Y are obtained as

$$\begin{aligned}
\mathcal{L}^{7/2^\pm}_{BYK} &= -\frac{g_{BKY}}{m_K^3}\bar{B}\Gamma^{(\mp)}Y^{\mu\nu\alpha}\partial_\mu\partial_\nu\partial_\alpha K + \text{ H.c.},\\
\mathcal{L}^{7/2^\pm}_{BYK\gamma} &= i\frac{g_{BYK}}{m_K^3}\bar{B}\Gamma^{(\pm)}Y^{\mu\nu}\hat{e}_K A_{\mu\nu}\bar{K} + \text{ H.c.}..
\end{aligned} \tag{17}$$

By analyzing the production amplitudes with an intermediate hyperon resonance on its mass shell, it was found that the production amplitudes have the following patterns [17]:

$$|M_{1/2^\pm}|^2 \propto (\varepsilon_N \mp m_N)(\varepsilon_\Xi \mp m_\Xi), \qquad |M_{3/2^\pm}|^2 \propto (\varepsilon_N \pm m_N)(\varepsilon_\Xi \pm m_\Xi). \tag{18}$$

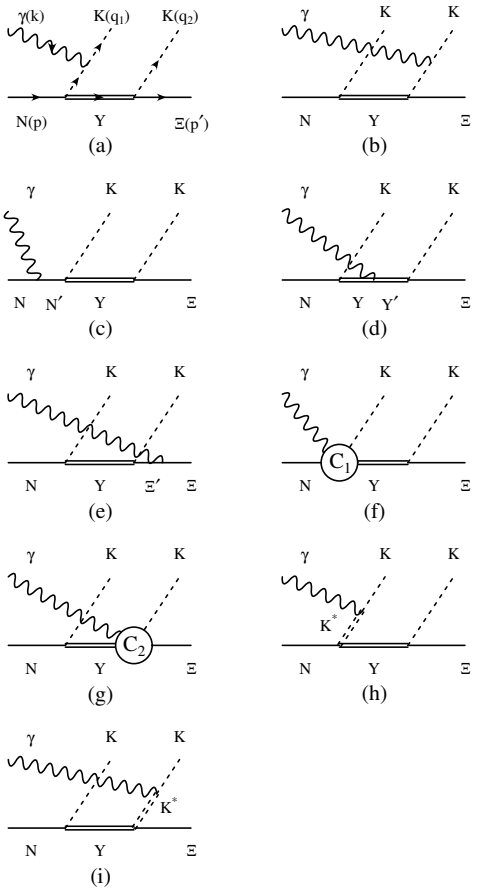

Fig. 4. Diagrams contributing to the reaction mechanism of $\gamma N \to KK\Xi$. The intermediate baryon states are denoted as N' for the nucleon and Δ resonances, Y, Y' for the Λ and Σ resonances, and Ξ' for $\Xi(1318)$ and $\Xi(1530)$. The intermediate mesons in the t-channel are K [(a) and (b)] and K^* [(h) and (i)]. The diagrams (f) and (g) contain the generalized contact currents that maintain gauge invariance of the total amplitude. Diagrams corresponding to (a)–(i) with $K(q_1) \leftrightarrow K(q_2)$ are also understood.

where M_{J^P} denotes the photoproduction amplitude involving the intermediate hyperon with the spin-parity J^P; $\varepsilon_i \equiv \sqrt{\boldsymbol{p}_i^2 + m_i^2}$ with $\boldsymbol{p}_i$ and m_i denoting the momentum and mass, respectively, of the nucleon or the Ξ as $i = N$ or Ξ. This proportionality is valid only when the intermediate hyperon lies on its mass shell, and it should not be applied to the low-mass resonances which are far off-shell in the reaction considered in the present work. Among the $J^P = 1/2^-$ and $3/2^+$ resonances listed in PDG, assuming the ΞYK coupling strength to be of the order of the NYK coupling strength, we find that only the $\Lambda(1800)1/2^-$ and the $\Lambda(1890)3/2^+$ resonances can contribute significantly. Therefore, only these two high-mass resonances were considered in the model of Ref. [17].

Furthermore, in Ref. [18], we confirm that these kinds of relationships are valid for higher-spin resonances; namely,

$$|M_{5/2^\pm}|^2 \propto (\varepsilon_N \mp m_N)(\varepsilon_\Xi \mp m_\Xi), \qquad |M_{7/2^\pm}|^2 \propto (\varepsilon_N \pm m_N)(\varepsilon_\Xi \pm m_\Xi). \tag{19}$$

Thus, we can consider the contributions only from the $J^P = 5/2^-$ and $7/2^+$ resonances. We then see from PDG that the $\Sigma(2030)7/2^+$, the $\Sigma(1775)5/2^-$, and the $\Lambda(1830)5/2^-$ are the only candidates. Among them the $\Sigma(1775)5/2^-$, and $\Lambda(1830)5/2^-$ have a mass below or very close to the threshold.

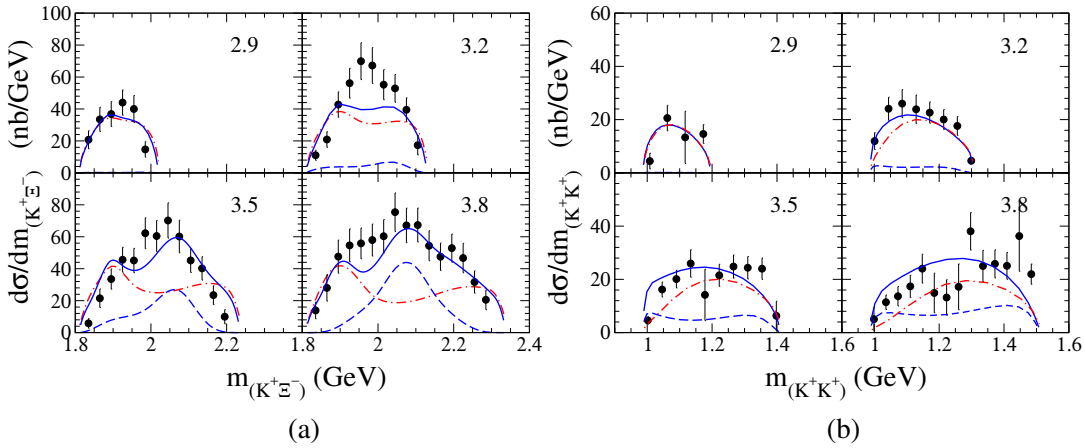

Fig. 5. Invariant mass distribution (a) of the $K^+\Xi^-$ pair and (b) of the K^+K^+ pair in the reaction of $\gamma p \to K^+K^+\Xi^-$. The number in the right upper corner of each graph indicates the incident photon energy in GeV. The dot-dashed lines are the results of Ref. [17] which includes only spin-1/2 and -3/2 hyperon resonances. The solid lines are the results of the present model, while the dashed lines show the contributions from the $\Sigma(2030)7/2^+$. Experimental data are from Ref. [19].

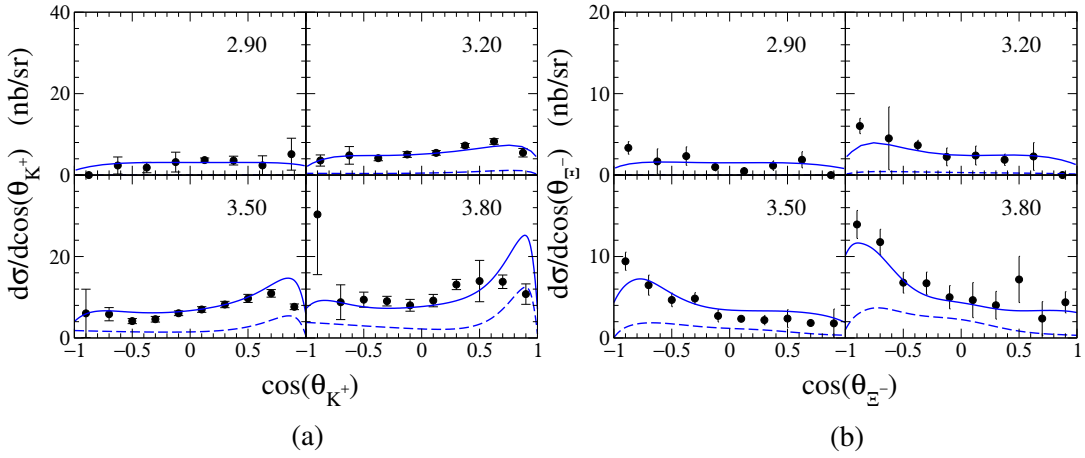

Fig. 6. Differential cross section (a) $d\sigma/d\cos(\theta_{K^+})$ and (b) $d\sigma/d\cos(\theta_{\Xi^-})$ for $\gamma p \to K^+K^+\Xi^-$. The number in the right upper corner of each graph indicates the incident photon energy in GeV. The solid lines are the full results of the present model, while the dashed lines show the contributions from the $\Sigma(2030)7/2^+$. Experimental data are from Ref. [19].

Since we are interested in the resonances of mass about 2 GeV, we focus on the role of the $\Sigma(2030)7/2^+$ resonances in order to analyze the data of Ref. [19]. We vary the coupling constants of the $\Sigma(2030)7/2^+$ to reproduce the measured data. In fact, we have verified explicitly that the inclusion of the spin-5/2 resonances mentioned above do not help eliminate the problem of the double-bump structure in the predicted $K^+\Xi^-$ invariant mass distribution mentioned before [18].

Our results for the invariance mass distributions of the $K^+\Xi^-$ pair and of the K^+K^+ pair in the reaction of $\gamma p \to K^+K^+\Xi^-$ are given in Fig. 5. In this figure, the dot-dashed lines are the results of Ref. [17], where only the $\Lambda(1800)1/2^-$ and $\Lambda(1890)3/2^+$ are included on top of the low-lying resonances. In contrast to the experimental data from the CLAS collaboration [19], which are given by the filled circles, this model yields a double-bump structure in the $K^+\Xi^-$ invariant mass distribution as illustrated in Fig. 5(a). As was discussed above, this feature evidently implies that the contribution from a resonance with a mass around 2 GeV is missing. As can be seen by the dashed lines in Fig. 5(a),

this can be attributed to the role of the $\Sigma(2030)$. When combined with the other terms, the double-bump structure appeared in the model of Ref. [17] is now absent as shown by the solid lines in Fig. 5(a). This leads us to conclude that the double-bump structure is an artifact of the previous model and that the $\Sigma(2030)$ of $J^P = \frac{7}{2}^+$ has a key role to make the model predictions to be in a fair agreement with the data. As expected, the contribution from the $\Sigma(2030)7/2^+$ resonance can hardly be seen at low energies with $E_\gamma \leq 3.2$ GeV. Therefore, the results of the present model are very similar to those of the model of Ref. [17] at these energies. However, at higher energies, the range of the invariant $K^+\Xi^-$ mass fully covers the mass region of the $\Sigma(2030)$ and the results show the prominent contribution from this resonance. Figure 5(b) shows the results for the invariant mass distribution of the K^+K^+ pair in the same reaction. Here again, the contribution from the $\Sigma(2030)$ resonance is large for higher photon energies. However, as in the model of Ref. [17], the obtained K^+K^+ invariant mass distribution does not show any structure because of the absence of the exotic $S = +2$ mesons.

In Fig. 6, we present the differential cross sections $d\sigma/d\cos(\theta_{K^+})$ and $d\sigma/d\cos(\theta_{\Xi^-})$ for $\gamma p \to K^+K^+\Xi^-$ obtained in this model. This again shows that the role of the $\Sigma(2030)$ becomes prominent as the incident photon energy increases and is crucial to reproduce the measured data for differential cross sections. In particular, $d\sigma/d\cos(\theta_{K^+})$ is forward-peaked and $d\sigma/d\cos(\theta_{\Xi^-})$ is backward-peaked, which supports the analyses of Ref. [17]. We confirm that the contribution from the $\Sigma(2030)$ also respects this behavior.

5 Summary and Discussion

Accumulation of precise data of scattering experiments at resonance energy region provides a good chance to search for missing resonances and to extract the properties of baryon resonances. Since many baryon resonances in this energy region, i.e., at masses of around 2 GeV, have higher spins, it is necessary to include them explicitly in a full coupled-channel calculation. This requires a unified relativistic treatment of meson and baryon fields of arbitrary spins. In this direction, we used the Fronsdal formalism for the propagators of high spin fields and applied it to the reactions of $\gamma p \to K\Sigma(1385)$ and $\gamma p \to K^+K^+\Xi^-$ to found that the role of higher spin resonances are important to understand the production mechanisms of hadron production reactions. Furthermore, in order to relate the coupling constants of effective Lagrangians to quark model predictions, it is needed to derive the explicit formulas for the partial decay amplitudes. It is, however, well known that there arises an ambiguity when the Rarita-Schwinger field is off the mass-shell. Although, for the coupling constants and their relationships to quark model prediction, this problem can be avoided as the hyperon is on-shell, the off-shell problem should be resolved and taken into account in order to fully understand the role of high spin resonances in the production mechanisms.

I am grateful to fruitful discussions with T.-S. H. Lee and K. Nakayama. This work was supported by Basic Science Research Program through the National Research Foundation of Korea (NRF) funded by the Ministry of Education, Science and Technology (Grant No. 2010-0009381).

References

1. K. Nakamura et al. (Particle Data Group), J. Phys. G **37**, 075021 (2010), http://pdg.lbl.gov
2. D.O. Riska, G.E. Brown, Nucl. Phys. A **679**, 577 (2001)
3. Y. Oh, A.I. Titov, T.S.H. Lee, Phys. Rev. C **63**, 025201 (2001)
4. A.I. Titov, T.S.H. Lee, Phys. Rev. C **66**, 015204 (2002)
5. V. Shklyar, G. Penner, U. Mosel, Eur. Phys. J. A **21**, 445 (2004)
6. R.E. Behrends, C. Fronsdal, Phys. Rev. **106**, 345 (1957)
7. C. Fronsdal, Nuovo Cim. Suppl. **9**, 416 (1958)
8. J.G. Rushbrooke, Phys. Rev. **143**, 1345 (1966)
9. S.J. Chang, Phys. Rev. **161**, 1308 (1967)
10. W. Rarita, J. Schwinger, Phys. Rev. **60**, 61 (1941)

11. Y. Oh, C.M. Ko, K. Nakayama, Phys. Rev. C **77**, 045204 (2008)
12. L. Guo, D.P. Weygand (CLAS Collaboration), *Photoproduction of $K^{*+}\Lambda$ and $K^{+}\Sigma(1385)$ in the reaction $\gamma p \to K^{+}\Lambda\pi^{0}$ at Jefferson Lab*, in *Proceedings of International Workshop on the Physics of Excited Baryons (NSTAR 05)*, edited by S. Capstick, V. Crede, P. Eugenio (World Scientific, Singapore, 2006), pp. 306–309, arXiv:hep-ex/0601010
13. K. Hicks et al. (LEPS Collaboration), Phys. Rev. Lett. **102**, 012501 (2009)
14. S. Capstick, W. Roberts, Phys. Rev. D **58**, 074011 (1998)
15. H. Kamano, M. Arima, Phys. Rev. C **69**, 025206 (2004)
16. Y. Oh, K. Nakayama, T.S.H. Lee, Phys. Rep. **423**, 49 (2006)
17. K. Nakayama, Y. Oh, H. Haberzettl, Phys. Rev. C **74**, 035205 (2006)
18. J.K.S. Man, Y. Oh, K. Nakayama, Phys. Rev. C **83**, 055201 (2011)
19. L. Guo et al. (CLAS Collaboration), Phys. Rev. C **76**, 025208 (2007)